Spectroscopic properties and mechanism of $Tm^{3+}/Er^{3+}/Yb^{3+}$ co-doped oxyfluorogermanate glass ceramics containing BaF_2 nanocrystals*

Hu Yue-Bo(胡曰博)[a], Qiu Jian-Bei(邱建备)[b]†, Zhou Da-Cheng(周大成)[b], Song Zhi-Guo(宋志国)[b], Yang Zheng-Wen(杨正文)[b], Wang Rong-Fei(王荣飞)[b], Jiao Qing(焦 清)[b], and Zhou Da-Li(周大利)[c]

[a] *Faculty of Mechanical and Electrical Engineering, Kunming University of Science and Technology, Kunming* 650500, *China*

[b] *Key Laboratory of Advanced Materials in Rare & Precious and Non-ferrous Metals, Ministry of Education, Key Laboratory of Advanced Materials of Yunnan Province, Faculty of Materials Science and Engineering, Kunming University of Science and Technology, Kunming* 650093, *China*

[c] *College of Materials Science and Engineering, Sichuan University, Chengdu* 610064, *China*

(Received 8 April 2013; revised manuscript received 27 April 2013; published online 10 December 2013)

Transparent $Tm^{3+}/Er^{3+}/Yb^{3+}$ co-doped oxyfluorogermanate glass ceramics containing BaF_2 nanocrystals are prepared. Under excitation of a 980-nm laser diode (LD), compared with the glass before heat treatment, the $Tm^{3+}/Er^{3+}/Yb^{3+}$ co-doped oxyfluorogermanate glass ceramics can emit intense blue, green and red up-conversion luminescence and Stark-split peaks; X-ray diffraction (XRD) and transmission electron microscope (TEM) results show that BaF_2 nanocrystals with an average diameter of 20 nm are precipitated from the glass matrix. Stark splitting of the up-conversion luminescence peaks in the glass ceramics indicates that Tm^{3+}, Er^{3+} and (or) Yb^{3+} ions are incorporated into the BaF_2 nanocrystals. The up-conversion luminescence intensities of Tm^{3+}, Er^{3+} and the splitting degree of luminescence peaks in the glass ceramics increase significantly with the increase of heat treat temperature and heat treat time extension. In addition, the possible energy transfer process between rare earth ions and the up-conversion luminescence mechanism are also proposed.

Keywords: up-conversion luminescence, oxyfluorogermanate glass ceramic, $Tm^{3+}/Er^{3+}/Yb^{3+}$co-doped, energy transfer

PACS: 42.70.–a

DOI: 10.1088/1674-1056/23/2/024205

1. Introduction

The up-conversion (UC) luminescence, until now, has been extensively investigated by using rare earth ions-doped glasses, due to their potential applications in fields such as solar cell, three-dimensional display, optical communication, solid-state laser, microscopic imaging, anti-counterfeit technology, sensors, etc.[1–6] As is well known, the UC efficiency depends largely on the host material for RE ions since host glass with low phonon energy can reduce the multiphonon relaxation and thus achieves strong UC luminescence.[7,8] Furthermore, to meet the requirements of practical applications, the chemical stability and mechanical intensity of host material should be high enough. Recently, RE ions-doped oxyfluoride glass ceramics containing fluoride crystals have attracted a great deal of attention.[9–13] Such materials combine the low phonon energy environment of fluoride crystals with the high chemical and mechanical stability of oxide glasses. In these glass ceramics, RE ions are preferentially incorporated into crystalline phases with phonon energy below 500 cm^{-1},[13] thus enabling the realization of strong UC luminescence. Wang and Ohwaki[14] confirmed that the UC luminescence efficiency of the transparent fluoroaluminosilicate glass ceramic containing YbF_3 and ErF_3 was about ten times stronger than that of an equally YbF_3 and ErF_3-doped fluoride glass. This high efficiency of UC was attributed to Er^{3+}-enriched $Pb_xCd_{1-x}F_2$ crystallites. Meng *et al.*[15] have reported on Er^{3+}/Yb^{3+}co-doped oxyfluoride glass and glass ceramics. It has been confirmed that RE ions enter into the nanoparticles using Judd–Ofelt theory and DTA analysis. Qiao *et al.*[16–18] have substituted alkaline-earth fluorides for poisonous agents such as CdF_2 and PbF_2 and have produced a series of Er^{3+}-doped transparent glass ceramics containing alkaline-earth fluoride nanocrystals. The results showed that the Er^{3+} and Yb^{3+} co-doped glass ceramics had higher luminescence efficiency than the precursor glass, too. So far, transparent oxyfluoride glass ceramics have been developed as ideal RE ions-doped hosts used for UC devices.

As far as oxyfluoride glass ceramics are concerned, the oxyfluorogermanate glass ceramic is one of the most promising hosts for RE ions because of its superior mechanical and thermal stability properties, lower phonon energy and high transparency in a wide wavelength range. Many research results concerning such a material have been reported.[19–23] In addition, BaF_2 is an important optical raw material with high solubilities of both sensitizer and activator RE ions and has

*Project supported by the National Natural Science Foundation of China (Grant Nos. 61265004 and 51272097) and the Specialized Research Fund for the Doctoral Program of Higher Education of China (Grant No. 20125314120018).

†Corresponding author. E-mail: qiu@kmust.edu.cn

© 2014 Chinese Physical Society and IOP Publishing Ltd

been used successfully as the crystal laser host.[24] Considering the advantages of the above two aspects, it can be expected that the RE ions-doped oxyfluorogermanate glass ceramics containing BaF_2 nanocrystals would show excellent photoluminescence properties. But as far as we know, there have been few studies on the spectroscopic properties and mechanism of RE ions-doped oxyfluorogermanate glass ceramics containing BaF_2 nanocrystals. In this article, the transparent $Tm^{3+}/Er^{3+}/Yb^{3+}$ co-doped GeO_2–AlF_3–BaF_2–GdF_3 (GABG) glass ceramics containing BaF_2 nanocrystals are investigated. The formation of BaF_2 nanocrystals in the glass ceramics is confirmed. The micro-morphology of nanocrystal is observed. Intense blue, green and red UC luminescence and Stark splitting of the Tm^{3+} and Er^{3+} UC luminescence peaks are observed, under the excitation of 980-nm LD. The dependence of up-conversion fluorescence intensity on excitation power in oxyfluorogermanate glass ceramics is investigated. The UC luminescence mechanism of the Tm^{3+} and Er^{3+} ions in the oxyfluorogermanate glass ceramic is discussed.

2. Experiment

The glass samples were prepared with the raw material of a purity of 99.99% and composition ratio in mol% of $60GeO_2{\cdot}10AlF_3{\cdot}25BaF_2{\cdot}1.93GdF_3{\cdot}3YbF_3{\cdot}0.02ErF_3{\cdot}0.05TmF_3$ by the conventional melting-quenching technique. For each batch, about 5 g of starting materials was thoroughly mixed in an agate mortar and then melted in a covered platinum crucible at 1300 °C for 30 min in a globar furnace under an Ar gas atmosphere. The glass melts were cast quickly into stainless steel plate which had been pre-heated and kept at around 280 °C. The obtained glass samples were annealed at the glass-transition temperature determined by differential thermal analysis (DTA) with the 10-K·min^{-1} heating rate under an air atmosphere. To obtain the glass ceramic samples, the glasses were reheated respectively at 595, 600, 605, 610 °C for 3 h and at 595 °C for 3, 4, 5, 6, 7 h.

DTA measurement was carried out in a DTG-60AH differential thermal analyzer in a temperature range from room temperature to 900 °C in order to confirm the glass transition temperature (T_g) and the crystallization peak temperature (T_c). X-ray diffraction (XRD) measurements were performed in a D8ADVANCE diffractometer with Cu-K_α radiation at 0.1°·min^{-1} scanning rate, 40-kV tube voltage and 40-mA tube current. The micro-morphology of nanocrystals was observed by a Philips EM420 transmission electron microscope (TEM) with an accelerating voltage of 120 kV. The UC emission spectra in a wavelength range from 390 nm to 760 nm were recorded with a HITACHI F-7000 Fluorescence spectrophotometer under 980-nm excitation with various powers. Optical transmittance spectra were recorded in a wavelength range from 300 nm to 2000 nm by a HITACHI U-4100 spectrophotometer. Specimens with the size of 4.0 mm×4.0 mm×1.2 mm with optically flat surfaces were used in the measurements. All the measurements were taken beginning from room temperature.

3. Results and discussion

Figure 1 shows the DTA curve of $Tm^{3+}/Er^{3+}/Yb^{3+}$ co-doped GABG glass. As seen from this figure, the glass transition takes place at around 585 °C and an obvious crystallized peak appears at 665 °C, centers at 677 °C and ends at 695 °C. In addition, it is found that the glass sample becomes opaque when it is heated over 610 °C. Therefore, to obtain transparent glass ceramics, the heat treatment temperature is selected to be in the range of 595 °C–610 °C.

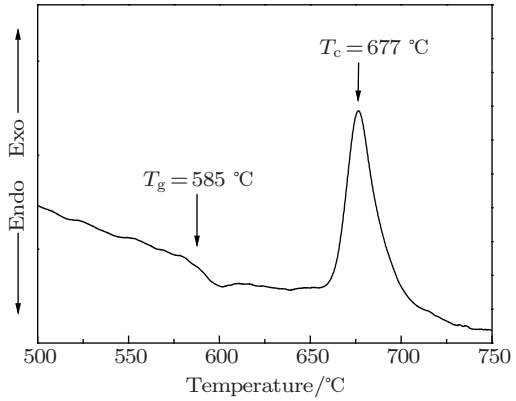


Fig. 1. The DTA curve of the $60GeO_2{\cdot}10Al_2O_3{\cdot}25BaF_2{\cdot}1.93GdF_3{\cdot}3YbF_3{\cdot}0.02ErF_3{\cdot}0.05TmF_3$ glass.

By XRD and TEM, the structures of $Tm^{3+}/Er^{3+}/Yb^{3+}$ co-doped GABG glass ceramics were analyzed. Figure 2 shows the XRD patterns of the precursor glass and glass ceramics obtained by heat treatment at 595 °C and 605 °C for 3 h, respectively. The precursor glass sample presents a broad diffraction curve characteristic of the amorphous state, while in the patterns of glass ceramics, four intense diffraction peaks are clearly observed, indicating that microcrystallites are successfully precipitated during thermal treatment. The diffraction pattern of the crystalline element is typical of a face-centered-cubic (fcc); these diffraction peaks around $2\theta = 25°$, 29°, 41°, and 49° can be assigned respectively to the (111), (200), (220) and (311) planes of the BaF_2 cubic phase. In addition, BaF_2 is also confirmed to be of the crystalline phase in our glass ceramics by energy dispersive X-ray spectroscopy (EDS) data obtained from TEM. As seen from the figure, with the increasing of heat treatment temperature, the diffraction peaks intensify obviously, suggesting that the mean size and crystalline fraction of glass ceramics are increased. An average crystal diameter is calculated from XRD patterns by using

the Debye–Scherrer equation[25] expressed by

$$D_{\rm hkl} = \frac{0.9\lambda \times 57.3}{\beta_{1/2}\cos\theta}, \quad (1)$$

where $D_{\rm hkl}$ is the crystal radius, λ is the X-ray wavelength, $\beta_{1/2}$ is the full-width at half-maximum (FWHM) of the diffraction peak, θ is the diffraction angle, 57.3 is a factor used to convert $\beta_{1/2}$ in degree into $\beta_{1/2}$ in radian. The obtained mean crystal sizes are about 18.9 nm and 19.4 nm for the glass ceramics prepared by heat treatment at 595 °C and 605 °C, respectively. On the other hand, the calculated values of lattice parameter (a) 0.5968 nm and 0.6036 nm on the XRD patterns of glass ceramics are less than the standard PDF value 0.6196 nm [PDF# 85-1341], indicating that the BaF_2 crystal lattice shrank after crystallization of the precursor glasses. This result could be ascribed to the incorporation of Tm^{3+}, Er^{3+} and (or) Yb^{3+} ions into the precipitated BaF_2 crystallite phase, because Ba^{2+} sites could be substituted by rare earth ions and their radius is smaller than that of Ba^{2+} ions.[26]

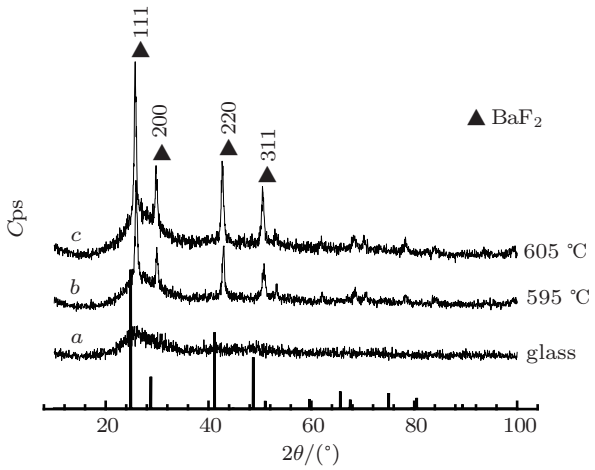


Fig. 2. XRD patterns of the $Tm^{3+}/Er^{3+}/Yb^{3+}$ co-doped GABG glass (curve *a*) and glass ceramics heated at 595 °C (curve *b*) and 605 °C (curve *c*) for 3 h.

The TEM image and the selected area electron diffraction (SAED) for the glass ceramic with heat treatment at 595 °C for 3 h are presented in Fig. 3. The TEM observations reveal that nearly spherical BaF_2 crystallites with a narrow particle-size distribution are homogeneously distributed among the glassy matrix. It has been known that such structural characteristics are important to determine the optical property of the glass ceramics.[27] The average diameter of the crystals precipitated is about 20 nm. From the SAED pattern, it follows that Laue diffraction spots with an obvious regular hexagon property are observed, confirming that the crystals are cubic-structured. These results are in good agreement with XRD data.

The transmittance spectra of $Tm^{3+}/Er^{3+}/Yb^{3+}$ co-doped GABG glass and glass ceramics heat-treated at 595 °C and 605 °C for 3 h in a spectral range from 300 nm to 2000 nm are exhibited in Fig. 4. The absorption bands corresponding to transitions from the ground to excited states for Tm^{3+}, Er^{3+} and Yb^{3+} ions, respectively, are indicated. Due to the influence of the band gap energy of a glass matrix, the absorption bands at wavelengths shorter than 350 nm could not be distinguished. The glass ceramics keep the transparency of precursor glass due to the sizes of precipitated nanocrystals being much smaller than the VIS-NIR wavelength. Furthermore, the absorbance intensity increases with the increasing of heat treatment temperature, suggesting that the enrichment concentration of rare earth ions in the grains increases. It is worth noting that the absorption around 980 nm increases up to 300% after crystallization, which is conducible to the pumping of glass ceramic by a common high-power laser diode (LD).

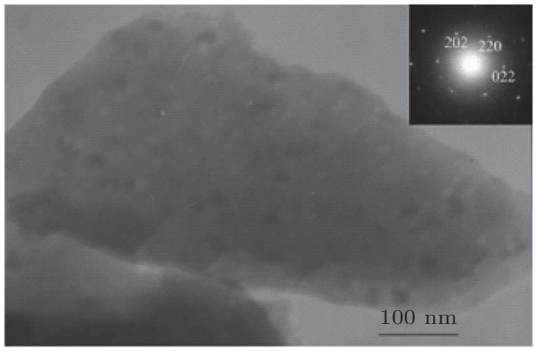


Fig. 3. TEM micrograph of the $Tm^{3+}/Er^{3+}/Yb^{3+}$ co-doped GABG glass ceramic heated at 595 °C for 3 h, with the inset showing the relevant selected area electron diffraction pattern.

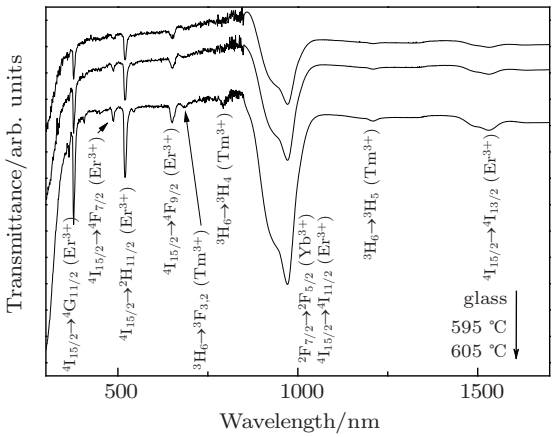


Fig. 4. Transmittance spectra of the $Tm^{3+}/Er^{3+}/Yb^{3+}$ co-doped GABG glass and glass ceramics.

Figure 5 shows the heat treatment temperature dependence of UC emission intensity in $Tm^{3+}/Er^{3+}/Yb^{3+}$ co-doped GABG precursor glass and glass ceramics with 3-h heat treatment under 980-nm excitation. It can be seen from the figure that the blue (477 nm), green (523 and 541 nm) and red (652 nm) emissions, which are identified as originating from $^1G_4 \rightarrow {}^3H_6$ (Tm^{3+}), ($^2H_{11/2}$, $^4S_{3/2}$) $\rightarrow {}^4I_{15/2}$ (Er^{3+}), and $^4F_{9/2} \rightarrow {}^4I_{15/2}$ (Er^{3+}) transitions, respectively, are simultaneously observed. Furthermore, it is found that the UC luminescence intensity of precursor glass is obviously weaker than those of glass ceramics. The inset shows that the variations of

541-nm and 652-nm emission intensity with the heat treatment temperature. As can be seen in the inset, the heat treatment dependence of $^4S_{3/2} \rightarrow {}^4I_{15/2}$ (Er^{3+}) transition is different from that of the $^4F_{9/2} \rightarrow {}^4I_{15/2}$ (Er^{3+}) transition. According to the Dexter theory, the dipole–dipole energy transfer (ET) rate is proportional to $1/R^6$, where R is the distance between the energy donor and the energy acceptor, suggesting that the ET rate depends on the distance between two rare earth ions. Therefore, the efficiency of ET UC quadratic power law depends on Er^{3+} concentration. As seen from the inset, the UC emission intensity of the $^4F_{9/2} \rightarrow {}^4I_{15/2}$ transition is linearly varied with the heat treatment temperature, whereas the emission intensity of the $^4S_{3/2} \rightarrow {}^4I_{15/2}$ transition increases in proportion to the square of the heat treatment temperature. This result indicates that the mechanism for green UC luminescence can be ascribed to the ET process and red UC luminescence may relate to excited state absorption (ESA);[5] the mechanism for the possible ET process is discussed in Fig. 8. At the same time, this result confirms the supposition that Tm^{3+}, Er^{3+} and Yb^{3+} ions are incorporated into BaF_2 nanocrystals after crystallization, which leads to the increase of local Er^{3+} concentration.

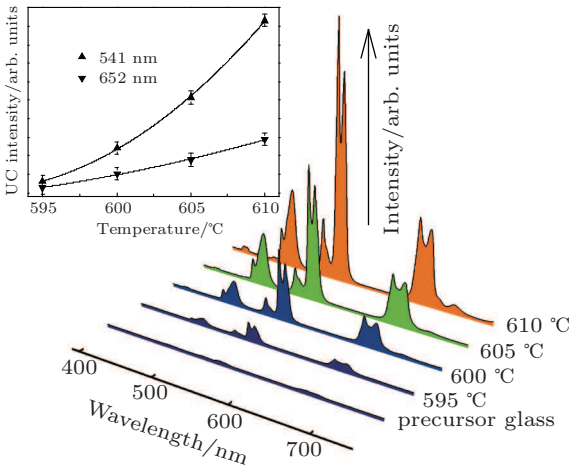


Fig. 5. (color online) Dependences of UC luminescence on heat treatment temperature for $Tm^{3+}/Er^{3+}/Yb^{3+}$ co-doped GABG glass and glass ceramics treated at temperatures of 595, 600, 605 and 610 °C for 3 h under 980-nm excitation. The inset shows that the changes of 541-nm and 652-nm emission intensity with heat treatment temperature.

Figure 6 shows the heat treatment time dependence of UC emission intensity in $Tm^{3+}/Er^{3+}/Yb^{3+}$ co-doped GABG glass ceramics treated at 595 °C under 980-nm excitation. It is seen from this figure that with the prolonging of heat treatment time, the UC luminescence intensities of Tm^{3+} and Er^{3+} ions gradually increase. As can be seen from Figs. 5 and 6, with the increasing of heat treatment temperature or heat treatment time, the UC luminescence intensity increases rapidly, which implies that heat treatment undoubtedly contributes to the UC luminescence of $Tm^{3+}/Er^{3+}/Yb^{3+}$ co-doped GABG glass ceramics. In addition, it is found that the Stark-splits of UC emission bands in glass ceramics become increasingly obvious, indicating that the enrichment concentration of rare earth ions in the grains increases with the increase of heat treatment time. It has been known that the UC luminescence of rare earth ions is usually baffled by the multi-phonon relaxation, which depends primarily on the energy gap between two successive levels and the phonon energy of the host. Generally, the lower the phonon energy of the host, the smaller the multi-phonon relaxation probability is.[28,29] The maximum phonon energy of BaF_2 (~ 346 cm^{-1} [30]) is much lower than that of oxide (the energy of Ge–O vibration is ~ 870 cm^{-1} [31]). Therefore, the precipitation of BaF_2 nanocrystals in glass ceramic and the entrance of Tm^{3+}, Er^{3+} or (and) Yb^{3+} into BaF_2 crystalline phase make the phonon energy decrease and the interdopant distances substantially shorten, which has an important effect on the ET rate between ions:[5] the energy conversion rate from Yb^{3+} to Tm^{3+}, Er^{3+} increases and the multi-phonon relaxation probability decreases in the glass ceramic. All of these result in intense UC luminescence.

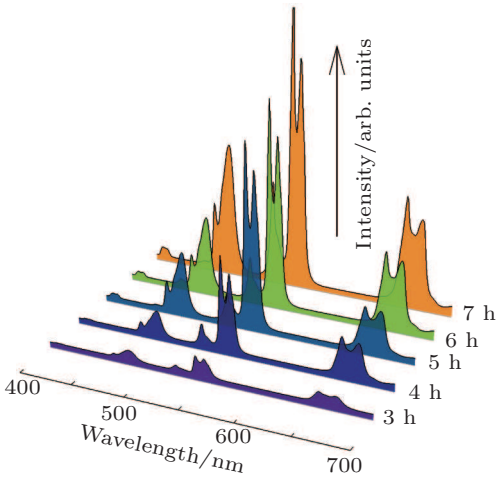


Fig. 6. (color online) Dependences of UC luminescence on heat treatment time for $Tm^{3+}/Er^{3+}/Yb^{3+}$co-doped GABG glass ceramics treated at 595 °C under 980-nm excitation.

In the frequency UC process, the UC emission intensity I_{UC} increases in proportion to the n-th power of the pumping power P, that is, $I_{UC} \propto P^n$, where n denotes the number of infrared (IR) photons absorbed per UC photon emitted.[32] A plot yields a straight line with slope n. Figure 7 shows log–log plots for the 477-nm, 523-nm, 541-nm, and 652-nm emissions in $Tm^{3+}/Er^{3+}/Yb^{3+}$co-doped GABG glass ceramic treated at 595 °C for 3 h. Values of 1.81, 1.78, 1.48, and 1.54 are obtained for the values of n corresponding to 477-nm, 523-nm, 541-nm, and 652-nm emission bands, respectively. The 477-nm, 523-nm, 541-nm, and 652-nm emissions bands exhibit approximately the law of quadratic power against excitation power, indicating that the mechanism for emissions of 477, 523, 541, and 652 nm is a typical two-photon process. In other words, two IR pump photons are needed in each of the blue, green and red UC emission.

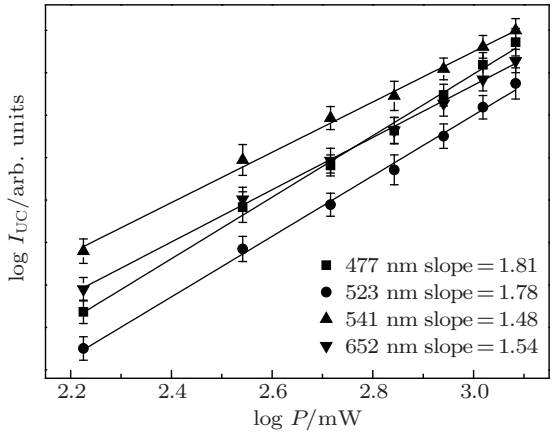


Fig. 7. Double-logarithmic plots of the dependence of UC fluorescence intensity on excitation power for $Tm^{3+}/Er^{3+}/Yb^{3+}$co-doped GABG glass ceramic treated at 595 °C for 3 h under 980-nm LD excitation.

The Tm^{3+} and Er^{3+} UC luminescence mechanisms in $Tm^{3+}/Er^{3+}/Yb^{3+}$ co-doped glasses, glass ceramics and UC inverse opal have been proposed in a previous report.[5,33–35] Based on the above results, the possible UC luminescence mechanisms for the blue, green and red emissions in the $Tm^{3+}/Er^{3+}/Yb^{3+}$ co-doped GABG glass ceramic under 980-nm excitation are proposed, as depicted in Fig. 8. For Tm^{3+} ions, a three-photon process for blue UC emission of Tm^{3+} was reported in $Tm^{3+}/Er^{3+}/Yb^{3+}$ co-doped GABG glass.[5] As far as we know, the two-photon blue UC emissions were observed only in the Yb–Er–Tm triply doped $Y_2Ti_2O_7$ UC inverse opal under a 980-nm excitation[35] and the Nd–Tm co-doped materials under a 793-nm excitation,[36,37] respectively. It is interesting that the two-photon process for Tm^{3+} blue UC emission is obtained in the $Tm^{3+}/Er^{3+}/Yb^{3+}$ co-doped GABG glass ceramic under a 980-nm excitation. The probable blue excitation process for the $^1G_4 \rightarrow {}^3H_6$ transition of Tm^{3+} can be explained as follows: first, Yb^{3+} is excited by 980-nm radiation, which corresponds to the Yb^{3+}:$^2F_{7/2} \rightarrow {}^2F_{5/2}$ transition. Subsequently, the energies of one Yb^{3+} ion transfer to one Tm^{3+} ion, resulting in the Tm^{3+}:$^3H_6 \rightarrow {}^3H_5$ excitation. The electrons in the excited state $^3H_5$ relax nonradiatively to the next $^3F_4$ level, then the electrons at the $^3F_4$ level can be excited to the $^1G_4$ level by ET through the route (Er^{3+}:$^4F_{9/2} \rightarrow {}^4I_{15/2}$) $\rightarrow$ (Tm^{3+}:$^3F_4 \rightarrow {}^1G_4$). The radiative transitions from the $^1G_4$ to $^3H_6$ could give a UC luminescence around 477 nm. The probable green (523 nm and 541 nm) and red (652 nm) excitation processes for the $^2H_{11/2} \rightarrow {}^4I_{15/2}$, $^4S_{3/2} \rightarrow {}^4I_{15/2}$, and $^4F_{9/2} \rightarrow {}^4I_{15/2}$ transitions of Er^{3+}, respectively, can be explained as follows: in the first step, the Er^{3+} $^4I_{11/2}$ level is directly excited with 980-nm light by ground state absorption (GSA) and/or by ET process from the $^2F_{5/2}$ level of Yb^{3+}:$^2F_{5/2}$ (Yb^{3+}) + $^4I_{15/2}$ (Er^{3+}) $\rightarrow$ $^2F_{7/2}$ (Yb^{3+}) + $^4I_{11/2}$ (Er^{3+}). The second step involves excitation processes based on the long-lived $^4I_{11/2}$ level as follows: ET from $^2F_{5/2}$ (Yb^{3+})+$^4I_{11/2}$ (Er^{3+}) $\rightarrow$ $^2F_{7/2}$ (Yb^{3+})+$^4F_{7/2}$ (Er^{3+}). The populated Er^{3+} $^4F_{7/2}$ level then relaxes rapidly and nonradiatively to the next lower levels $^2H_{11/2}$ and $^4S_{3/2}$ resulting from the small energy gap between them. The above processes then produce the two $^2H_{11/2} \rightarrow {}^4I_{15/2}$ and $^4S_{3/2} \rightarrow {}^4I_{15/2}$ green emissions centered at 523 nm and 541 nm, respectively. The red emission entered at 652 nm originates from the $^4F_{9/2} \rightarrow {}^4I_{15/2}$ transition. The population of $^4F_{9/2}$ is based on the processes as follows: first, as indicated above, the Er^{3+} $^4I_{11/2}$ level is excited. Subsequently, the $^4I_{13/2}$ level is populated, owing to the nonradiative relaxation from the upper $^4I_{11/2}$ level. The second step involves the excitation process as follows: ESA $^4I_{13/2}$ (Er^{3+}) + a photon$\rightarrow$ $^4F_{9/2}$ (Er^{3+}). Finally, there is the energy release process: the Er^{3+}:$^4F_{9/2} \rightarrow {}^4I_{15/2}$ radioactive transition takes place, giving a UC luminescence around 652 nm.

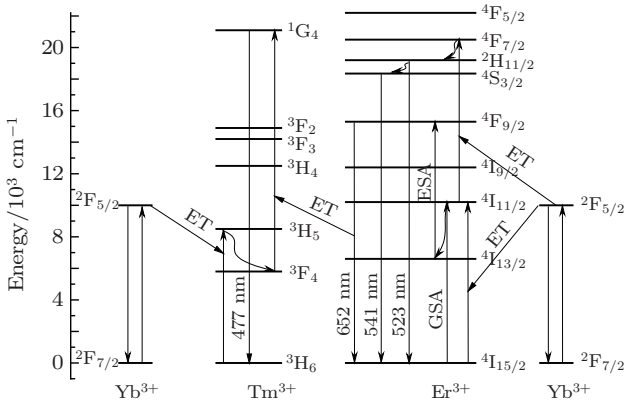


Fig. 8. Energy levels of Tm^{3+}, Er^{3+}, and Yb^{3+} and possible transition pathways in $Tm^{3+}/Er^{3+}/Yb^{3+}$co-doped GABG glass ceramics.

4. Conclusions

The $Tm^{3+}/Er^{3+}/Yb^{3+}$ co-doped oxyfluoride glass ceramics are synthesized in the compositions of $60GeO_2{\cdot}10Al_2O_3{\cdot}25BaF_2{\cdot}1.93GdF_3$. XRD patterns and EDS data reveal that the crystalline products precipitated in glass ceramics are BaF_2 crystalline materials. The glass ceramics present high transparency due to the sizes of the precipitated nanocrystals being small enough. The obvious Stark-split peaks are observed in the UC luminescence spectra of the glass ceramics, indicating that Tm^{3+}, Er^{3+} and (or) Yb^{3+} have been incorporated into the BaF_2 crystal lattices. In addition, it is confirmed that: the heat treatment process plays an important role in increasing the UC luminescence intensity, all of the four emissions in this work are due to typical two-photon processes, the mechanism for red UC luminescence can be ascribed to the ESA process and the mechanism for green UC luminescence may relate to the ET process. These results confirm that the formation of BaF_2 nanocrystals promotes the UC luminescence of rare earth ions. Our study results indicate that the transparent oxyfluorogermanate glass ceramics containing

BaF_2 nanocrystals have a broad application prospect in the optical instrument field.

References

[1] Li X P, Chen B J, Shen R S, Zhang J S, Sun J S, Cheng L H, Zhong H Y, Tian Y, Fu S B and Du G T 2013 *Chin. Phys. B* **22** 023202

[2] Hu Y B, Zhang X N, Zhou D L, Jiao Q, Wang R F, Huang J F, Long X B and Qiu J B 2012 *Spectroscopy and Spectral Analysis* **32** 56 (in Chinese)

[3] Zheng T, Qin J M, Jiang D Y, Lu J W and Xiao S C 2012 *Chin. Phys. B* **21** 043302

[4] Li C R, Li S F, Dong B, Cheng Y Q, Yin H T, Yang J and Chen Y 2011 *Chin. Phys. B* **20** 017803

[5] Hu Y B, Qiu J B, Zhou D L, Song Z G and Yang Z W 2011 *J. Wuhan University of Technology: Mater. Sci. Ed.* **26** 393

[6] Hu Y B, Qiu J B, Zhou D L, Yang Z W and Song Z G 2010 *J. Inorg. Mater.* **25** 551

[7] Chivian J S, Case W E and Eden D D 1979 *Appl. Phys. Lett.* **35** 124

[8] Dai S X and Zhang J J 2004 *Chin. Phys.* **13** 1156

[9] Dominiak-Dzik G, Lisiecki R, Ryba-Romanowski W and Krajczyk L 2012 *J. Alloys Compd.* **511** 189

[10] Prituzhalov V A, Ardashnikova E I, Vinogradov A A, Dolgikh V A, Videau J J, Fargin E, Abakumov A M, Tarakina N V and Tendeloo G V 2011 *J. Fluorin. Chem.* **132** 1110

[11] Zhao S L, Xu S Q, Jia G H, Deng D G, Huang L H and Wang H P 2011 *Mater. Lett.* **65** 2407

[12] Yu Y L, Chen D Q, Ma E, Wang Y S and Hu Z J 2007 *Spectrochim. Acta, Part A* **67** 709

[13] Xu W, Li C R, Cao B S and Dong B 2010 *Chin. Phys. B* **19** 127804

[14] Wang Y H and Ohwaki 1993 *J. Appl. Phys. Lett.* **63** 3268

[15] Meng J, Zhao L J, Yu H, Tang L Q, Liang Q, Yu X Y, Tang B Q, Su J and Xu J J 2005 *Acta Phys. Sin.* **54** 1442 (in Chinese)

[16] Qiao X S, Fan X P, Wang J and Wang M Q 2005 *J. Non-Cryst. Solids* **351** 357

[17] Qiao X S, Fan X P, Wang J and Wang M Q 2006 *J. Appl. Phys.* **99** 074302

[18] Qiao X S, Fan X P, Wang M Q and Wang J 2006 *Scr. Mater.* **55** 211

[19] Pan Z, Ueda A, Mu R and Morgan S H 2007 *J. Lumin.* **126** 251

[20] Gouveia-Neto A S, Costa E B, Bueno L A and Ribeiro S J L 2004 *J. Lumin.* **110** 79

[21] Zhao G L, Xi H D, Li X M, Wang J X and Han G R 2011 *J. Non-Cryst. Solids* **357** 2332

[22] Xiao Z H and Wang S L 2011 *Mater. Sci. Forum* **663–665** 1285

[23] Klimesz B, Dominiak-Dzik G, Żelechower M and Ryba-Romanowski W 2008 *Opt. Mater.* **30** 1587

[24] Kaminskii A A 1996 *A Laser Crystals: Their Physics and Properties*, 4th edn. (New York: Springer) p. 3

[25] Qiu J B, Kawamoto Y and Zhang J J 2002 *J. Appl. Phys.* **92** 5163

[26] Qiao X S, Fan X P, Wang M Q and Zhang X H 2008 *J. Non-Cryst. Solids* **354** 3273

[27] Tick P A 1998 *Opt. Lett.* **23** 1904

[28] Weber M J 1968 *Phys. Rev.* **171** 283

[29] Reisfeld R, Boehm L, Eckstein Y and Lieblich N 1975 *J. Lumin.* **10** 193

[30] Pollack S A and Chang D B 1988 *J. Appl. Phys.* **64** 2885

[31] Shen J K, Wu X L, Bao X M, Yuan R K, Zou J P and Tan C 2000 *Phys. Lett. A* **273** 208

[32] Suyver J F, Aebischer A, Garcia-Revilla S, Gerner P and Gudel H U 2005 *Phys. Rev. B* **71** 125123

[33] Xu S Q, Ma H P and Fang D W 2005 *Mater. Lett.* **59** 3066

[34] Tikhomirov V K, Driesen K, Görller-Walrand C and Mortier M 2008 *Mater. Sci. Eng. B* **146** 66

[35] Yan D, Zhu J L, Wu H J, Yang Z W, Qiu J B, Song Z G, Yu X, Yang Y, Zhou D C, Yin Z Y and Wang R F 2012 *J. Mater. Chem.* **22** 18558

[36] Lahoz F, Shepherd D P, Wilkinson J S and Hassan M A 2008 *Opt. Commun.* **281** 3691

[37] Chung W J and Heo J 2001 *J. Am. Ceram. Soc.* **84** 348